Rare Metal Materials and Engineering
Volume 52, Issue 9, September 2023
Available online at www.rmme.ac.cn

Science Press

Cite this article as: Xiao Bang, Jia Wenpeng, Wang Jian, et al. Review on Additively Manufactured Refractory High-Entropy Alloys[J]. Rare Metal Materials and Engineering, 2023, 52(09): 3056-3064.

REVIEW

Review on Additively Manufactured Refractory High-Entropy Alloys

Xiao Bang[1,2], Jia Wenpeng[1], Wang Jian[1], Zhou Lian[1,2]

[1] State Key Laboratory of Porous Metal Materials, Northwest Institute for Nonferrous Metal Research, Xi'an 710016, China; [2] State Key Laboratory of Solidification Processing, Northwestern Polytechnical University, Xi'an 710072, China

Abstract: Searching for printable metallic materials is of great importance. In recent years, several kinds of printable alloys have been researched, such as Ti-6Al-4V, FeMnCoCrNi, stainless steels, and some refractory high-entropy alloys (RHEAs). In spite of these delightful results, the development in additive manufacturing of RHEAs is proceeding slowly. Because of the excellent behavior of RHEAs at high temperatures, more requirements are proposed for the complex shape forming. This review primarily introduced the recent studies on additive manufacturing of RHEAs. The laser beam-based, electron beam-based, and wire-based additive manufacturing techniques for fabrication of RHEAs were summarized. In addition, the opportunities and challenges of the current development of RHEAs fabricated by additive manufacturing were discussed.

Key words: additive manufacturing; refractory high-entropy alloy; laser beam-based deposition system; electron beam-based melting system; microstructure; mechanical properties

Refractory high-entropy alloys (RHEAs) usually consist of elements with elevated melting temperatures, such as Hf, Mo, Nb, Ta, W, Zr, V, Cr, and Ti[1–2]. Senkov et al[3–4] firstly investigated the microstructure and mechanical properties of the emerged WMoTaNb RHEAs. Because of their excellent high-temperature behavior, RHEAs, including WMoTaNb[4], WMoTaNbV[4], $NbCrMo_{0.5}Ta_{0.5}TiZr$[5], and HfNbTaTiZr[6], are of great application importance in aerospace, nuclear reactors, and power industries. However, most RHEAs suffer from the serious brittleness, high hardness, and difficulties in subsequent deformation process, which severely restrict their further applications[3,7–9].

Additive manufacturing, including powder-bed systems, powder-feed systems, and wire-feed systems, is suitable to fabricate the customized parts with complex geometries through the assistant of computer-aided design[10]. Recently, there are three representative and prevalent techniques of additive manufacturing: wire-based additive manufacturing, direct energy deposition (DED), and selective electron beam melting (SEBM)[10–12], as shown in Fig.1. Generally, the additive manufacturing techniques involve the high-energy beams (electron and laser beams). Interactions between energy beams and powders or wires can efficiently form the melt pools, i.e., the material can be rapidly transformed into liquid. The cyclic melting-solidification can form the components layer by layer.

RHEAs have strong thermal resistance during deformation at extremely high temperatures, which endows RHEAs with particular charm during their service as nuclear and aerospace engines. Additionally, the fast development of these fields requires the parts with complex shapes for high efficiency. Hence, searching for RHEAs with considerable printability is of great urgency. In this review, forming methods, microstructures, mechanical properties, and problems of RHEAs manufactured by additive manufacturing techniques were discussed.

1 Additive Manufacturing Techniques

1.1 Laser beam-based deposition

Kunce et al[13] deposited TiZrNbMoV RHEAs by laser engineered net shaping (LENS) method, which was conducted in the early period of additive manufacturing investigation. With the development of 3D printing, more RHEAs with considerable printability have been manufactured. DMD, SLM, LCD, and LMD denote the direct metal deposition, selected laser melting, laser cladding deposition, and laser metal deposition, respectively. As listed in Table 1, the laser

Received date: March 29, 2023
Corresponding author: Wang Jian, Ph. D., Professor, State Key Laboratory of Porous Metal Materials, Northwest Institute for Nonferrous Metal Research, Xi'an 710016, P. R. China, Tel: 0086-29-86231095, E-mail: jwangxjtu@163.com

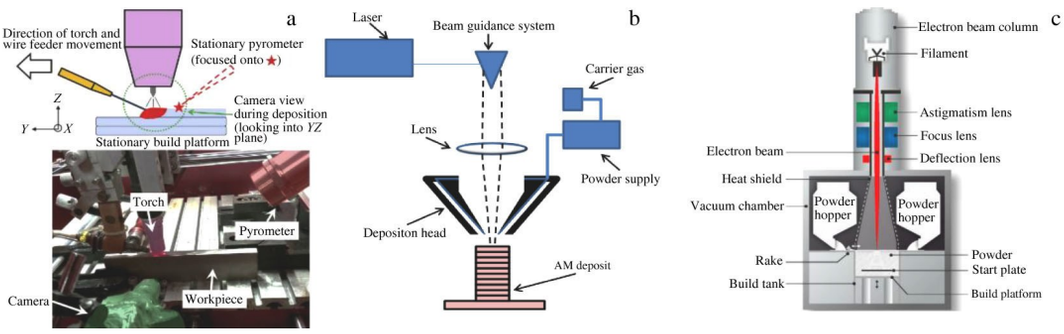

Fig.1 Schematic diagrams of the representative additive manufacturing techniques: (a) wire-based additive manufacturing[10]; (b) DED[11]; (c) electron beam melting system[12]

beam-assisted additive manufacturing consists of in-situ alloying (DED and LMD[18–19,24,26,28,30–31]) and powder-bed fusion[15,17,20–23] of refractory elements.

Because the powder conditions of DED, LMD, and SLM techniques are different, the laser powers for melting these refractory elements are always at different levels. It is clear that LMD or DED usually involves high melting power, whereas SLM involves the low melting power. Besides, the scanning speed of DED or LMD techniques is lower than 10 mm/s, whereas that of SLM technique is quite fast of above 100 mm/s. These characteristics indicate that LMD and DED have the similar melting processes (in-situ alloying and powder melting), which require larger linear energy density, compared with SLM technique. Such deviations in linear energy density are related to the laser power, powder-energy beam interaction, and atmosphere (vacuum or flowing gas).

Table 1 Laser-assisted additive manufacturing of RHEAs

RHEA system	Method	Laser power/W	Scanning speed/mm·s^{-1}	Ref.
WMoTaNb	DMD	800	2.5	[14]
WMoTaNb	SLM	400	250	[15]
WMoTaNb	LCD	565	8	[16]
WMoTaNb	SLM	500	250	[17]
WMoTaNb	DED	1800	5	[18]
WMoTaNb	DED	800	4.2	[19]
WMoTaNbV	SLM	100–600	100–1600	[20]
WMoTaNbV	SLM	320	200–800	[21]
C/WMoTaNb	SLM	400	200	[22]
TiC/WMoTaNbV	SLM	325	200–700	[23]
TiZrNbTa	LMD	500–3500	1.6–3.3	[24]
NbMoTaNiTi	SLM	300	300	[25]
MoNbTiV	DED	260	200	[26]
TiNbTaZrMo	SLM	300	1000	[27]
NbMoTaTiZrAl	DED	5000	150	[28]
NbTaTiMo	SLM	320	500	[29]
TiZrNbHfTa	LMD	1200	-	[30]
TiZrNbHfTa	LMD	2900	-	[31]

1.2 Electron beam-based melting

Different from the laser beam-assisted additive manufacturing, the electron beam-based melting with representative SEBM technique is occasionally employed in the RHEAs manufacturing. The high-energy electron beam melted refractory alloys normally have high efficiency, such as TiZrNbTa[32], $Mo_{20}Nb_{20}Co_{20}Cr_{20}(Ti_8Al_8Si_4)$[33], WMoTaNb[34], and WTaRe[35]. AlCrMoNbTa RHEA can be prepared by SEBM[36]. Fig. 2a and 2b show the key steps of AlCrMoNbTa RHEA during SEBM process[36]: the pre-sintering of powders and electron beam melting of powders. As shown in Fig. 2c and 2d, the as-deposited RHEA samples have rough morphologies with shining metallic upper surfaces, and some samples even exhibit curved boundaries, suggesting the over-melted state. Because the refractory elements have high melting points, higher linear energy densities are usually required in parameter-designing in order to totally melt the mixed powders.

Besides, the WMoTaNb-based RHEAs have printability in some extent[37–38]. With suitable processing parameters, the surface conditions and internal microstructures can be substantially optimized. This result indicates that SEBM is a powerful method in RHEA manufacturing with large solidification temperature ranges (W: 3410 °C; Ti: 1668 °C).

1.3 Other additive manufacturing techniques

Wire arc additive manufacturing (WAAM), as one of the wire-based additive manufacturing techniques, can form electric arc between tungsten electrode and substrate, therefore melting the feeding wires. WAAM is similar to DED in beam-powder interactions. Instead of powder[39], WAAM uses wire, which can totally melt the feeding materials without waste, thus presenting great potential in environment-friendly applications. Due to the high forming efficiency, high material utilization ratio, and large manufactured part size, WAAM is commonly employed, compared with the laser- and electron beam-based additive manufacturing techniques[40–41], for the manufacture of refractory metals (Mo and W alloys)[42–43]. However, the RHEA manufacturing is rarely reported. Only RHEAs, such as MoNbTaWTi[44] and $Nb_{37.7}Mo_{14.5}Ta_{12.6}Ni_{28.16}Cr_{7.04}$[45], have been manufactured by WAAM method. The underlying reasons may be the high cost and difficulty in manufacture of appropriate wires for WAAM.

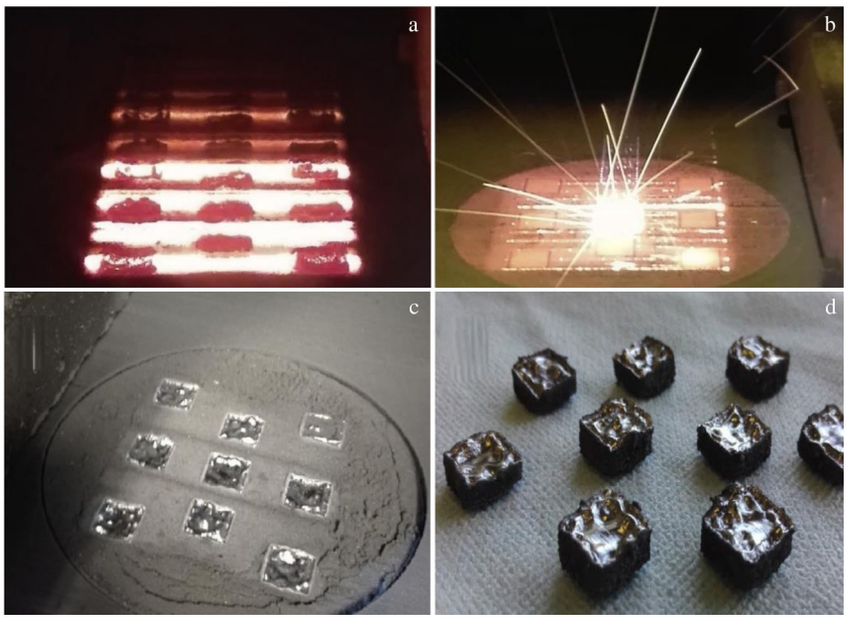

Fig.2 SEBM process of AlCrMoNbTa RHEAs[36]: (a) preheating or powder pre-sintering; (b) powder melting; (c) formed samples before removing from substrate; (d) as-deposited samples

Fig.3a shows the appearance of WAAM feeding wire, which is used for the laser melting process, as shown in Fig. 3b. Before the formation of thin walls, a layer-by-layer deposition is required and the cross-sectional morphologies of deposited lines are shown in Fig.3c. Fig.3d shows the as-deposited thin wall, and Fig.3e shows the appearance of changing bead at the start and end portions of thin wall. Fracture frequently occurs in RHEAs with high brittleness. The deposition process is always accompanied by high moving laser speeds (m/min) and high power (above 1000 W). Therefore, WAAM is an excellent method to manufacture RHEAs.

2 Microstructures of As-Deposited RHEAs

The additive manufacturing of refractory elements involves

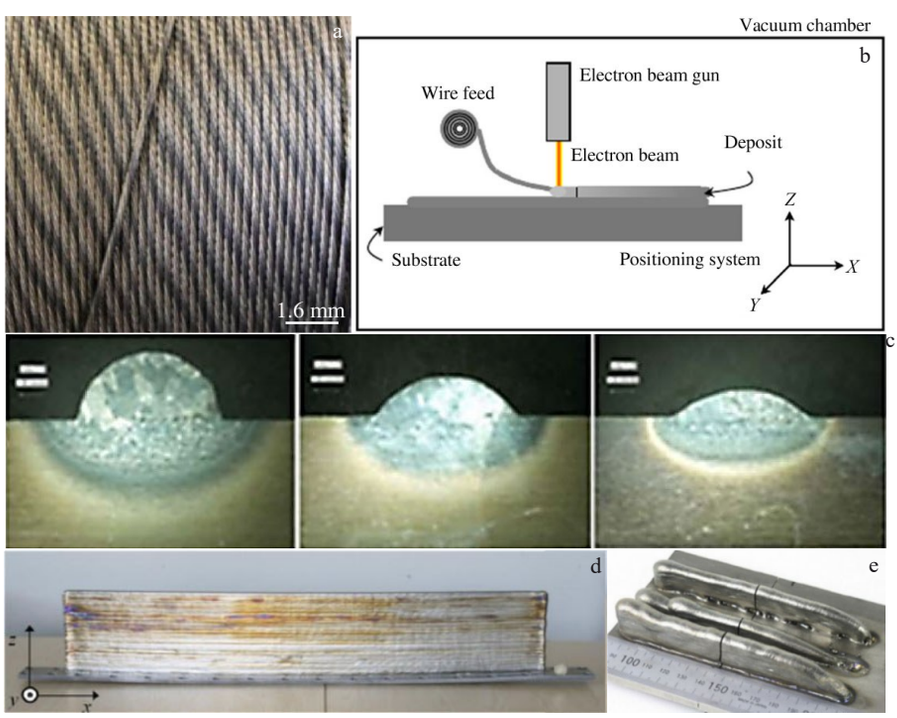

Fig.3 Appearance of WAAM feeding wire[45] (a); schematic diagram of WAAM process[46] (b); cross-sectional morphologies of deposited lines[47] (c); appearance of as-deposited wall[41] (d); appearance of changing bead at start and end portions of thin wall[48] (e)

the interactions between powders and high-energy beams[49–50]. During this stage, the powders absorb energy from the incident beam and melt pool, as shown in Fig.4a and 4b.

After the melting stage, the melt pool begins to solidify. Solidification of the refractory alloys seems different from that of the alloys with relatively lower melting points. High melting point suggests the early solidification of the melt pool, whereas the rapid cooling speed in additive manufacturing leaves the large thermal gradients in the as-deposited RHEAs. Because of their sluggish diffusion, high-entropy effect, and large energy barriers, these refractory elements start to diffuse. Thus, RHEAs maintain the thermally stable body-centered cubic (bcc) phase after formation[51].

The microstructures of representative WMoTaNb-based RHEAs are shown in Fig.5. According to Fig.5a, some cracks with large size in length and width appear in the single track. It is worth noting that almost all cracks are initiated from the outer surface at the part-powder interface. As shown in Fig.5b and 5b$_1$, the microstructures of the as-deposited WMoTaNbV bulk RHEAs are formed at scanning speed of 800 and 600 mm/s, respectively. Although changing the scanning speeds can alter cracking, cracks still exist in the as-deposited microstructures, indicating that the cracking is a serious problem in additively manufactured RHEAs, particularly in

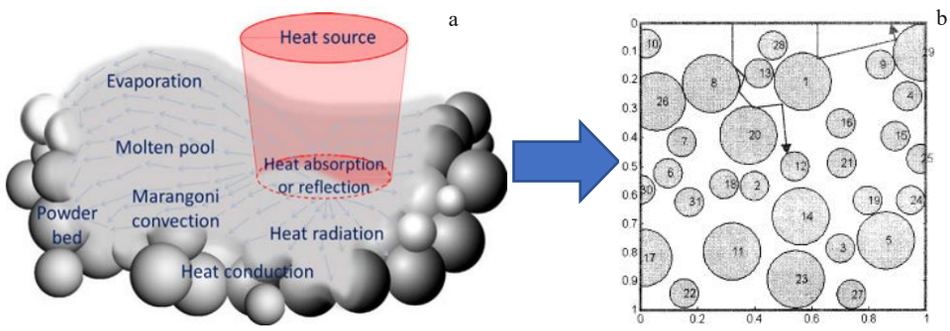

Fig.4 Schematic diagrams of powder-laser interactions: (a) melt pool[49]; (b) inter-reflection of laser beam and heat absorption by powder[50]

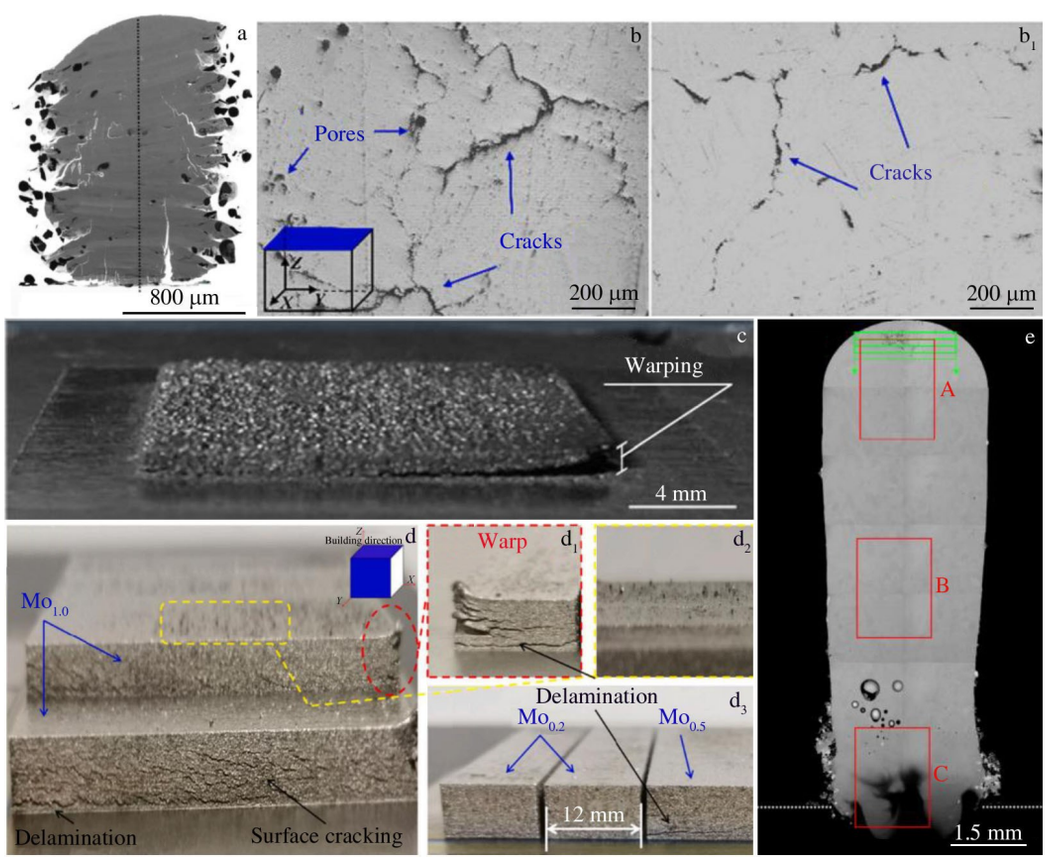

Fig.5 Microstructures of laser beam-assisted additive manufacturing: (a) microstructure of WMoTaNb RHEA by DED[14]; (b, b$_1$) microstructures of WMoTaNbV RHEA by SLM[21]; (c) warping of WMoTaNb RHEA by SLM[15]; (d, d$_1$–d$_3$) cracking and delamination phenomena in as-deposited NbTaTiMo RHEA by laser powder bed melting[29]; (e) microstructure of TiZrNbHfTa RHEA by LMD[31]

the WMoTaNb-based RHEAs. Fig. 5c and 5d show the warping, cracking, and delamination phenomena between the substrate and part, suggesting an accumulation of thermal stress at the edge of bulk WMoTaNb RHEA[15]. Moreover, the aggravation of warping leads to the unevenly spread of new powder layer. Delamination between layers deposited above the substrate also occurs, which not only causes cracks on RHEA surface, but also induces failure to RHEA before practical application.

Different from those normal cracking behavior in the aforementioned RHEAs, TiZrNbHfTa alloy is a ductile RHEA at room and elevated temperatures[52–53]. Several kinds of RHEAs are produced based on TiZrNbHfTa RHEA. It is worth noting that TiZrHfNbTa RHEA fabricated by LMD is free from cracking (Fig.5e). Only a few pores appear near the base plate[31]. Other RHEAs fabricated by laser-assisted additive manufacturing, including $Zr_{45}Ti_{31.5}Nb_{13.5}Al_{10}$[54] and TiZrHfNb[55], also have cracking-free microstructures. Thus, it can be deduced that RHEAs with good room- and high-temperature deformability may have good laser-dominated printability.

Electron beam-assisted additive manufacturing can be used to manufacture WMoTaNb-based[38], TiZrNbTa[32], and $Al_{0.5}CrMoNbTa_{0.5}$[36] RHEAs. Fig. 6a and 6b show the microstructures of WMoTaNbVFeCoCrNi RHEAs by SEBM. It can be clearly seen that some cracks with different features exist in the microstructure of as-deposited WMoTaNbVFeCoCrNi RHEA. These cracks with zigzag edges are caused by the lack of feeding flow in the interdendritic region during the last stage of solidification. When the temperature decreases, the solidification shrinkage and thermal contraction are initiated and exacerbate the cracking phenomenon in the mushy zone with uniaxial tensile stress[56]. Fig.6b and $6b_1$ display the cracking at the boundaries of two neighboring grains. Similar to the cracking mechanism in Ni-based alloy, the poor liquid feeding and the departure of two neighboring grains caused by tensile stress induce these solidification cracks[57], as shown in Fig.6c, $6c_1$, and $6c_2$.

In addition to these additively manufactured WMoTaNb-based RHEAs, TiZrNbTa and $Al_{0.5}CrMoNbTa_{0.5}$ RHEAs show better microstructures without significant cracking after electron beam-assisted additive manufacturing. Fig. 7a shows the microstructure of as-deposited TiZrNbTa RHEA, where pores can be clearly observed in the interdendritic regions. As shown in Fig. 7b, the microstructure of $Al_{0.5}CrMoNbTa_{0.5}$ RHEA prepared by SEBM consists of pores which are almost uniformly distributed in the grains.

Therefore, it can be concluded that the cracking and pores are the two main defects to influence the printability of additively manufactured RHEAs, particularly for the WMoTaNb-based RHEAs. TiZrNbHfTa-based RHEA exhibits quite good printability, which may stem from its excellent room temperature ductility. Hence, developing more ductile RHEAs is extremely urgent.

3 Mechanical Properties

Because RHEAs have high hardness and room-temperature brittleness, the characterization of their mechanical properties mainly focuses on the compression strength[3–4]. Hitherto, few RHEAs have tensile strength and ductility, such as NbZrTi-based, TiZrNbHfTa, TiZrNbHfTa-based RHEAs after several treatments[58–61]. Recently, Gou et al[55] reported the additively

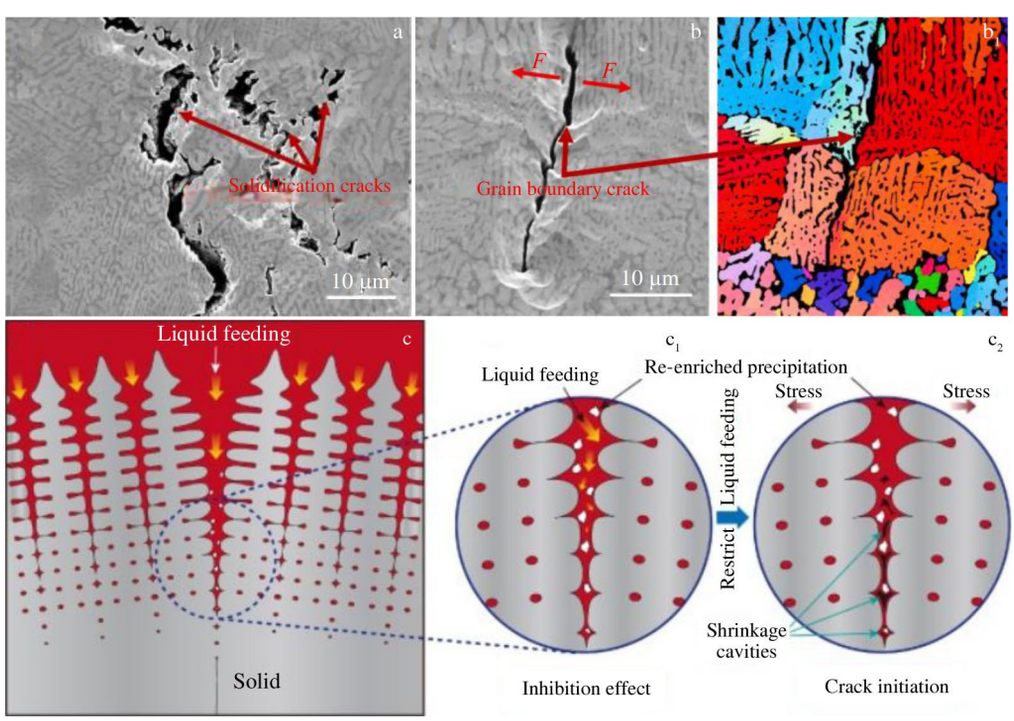

Fig.6 Microstructures of WMoTaNbVFeCoCrNi RHEAs by SEBM[38] (a, b, b_1); schematic diagrams of cracking mechanism[57] (c, c_1, c_2)

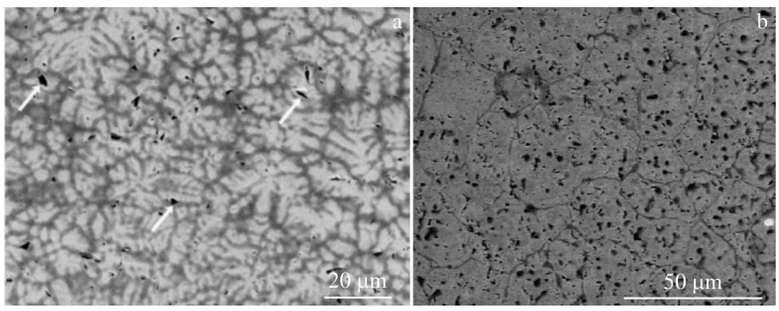

Fig.7 Microstructures of RHEAs: (a) TiZrNbTa RHEA by electron beam welding[32]; (b) $Al_{0.5}CrMoNbTa_{0.5}$ RHEA by SEBM[36]

manufactured TiZrHfNb RHEA has yield strength and elongation of about 1034 MPa and 18.5%, respectively. All these NbZrTi-based RHEAs shed light on new ways for the development of RHEAs by additive manufacturing techniques. However, when it comes to the WMoTaNb-based RHEAs, the compression performance is still in the dominant position. Therefore, searching for more printable RHEAs is pressingly necessary. Qi et al[62] suggested a method of tuning intrinsic ductility of bcc refractory alloys by alloying with group IV or V transition metals. Therefore, new RHEAs, such as WMoTaNbTi RHEAs, with considerable ductility are designed[63–65]. The WMoTaNbTi RHEA prepared by SEBM exhibits considerable mechanical properties[37].

Additively manufactured RHEAs always have serious defects in their microstructures, which severely weaken their mechanical behavior. To clearly identify the mechanical behavior of RHEAs, the hardness and compressive strength of these additively manufactured RHEAs are presented in Table 2 and Fig. 8. Compared with the as-cast WMoTaNb RHEA[3], these additively manufactured WMoTaNb or WMoTaNb-based RHEAs possess higher hardness, which is attributed to the enhanced solid-solution strengthening mechanism during rapid cooling process of additive manufacturing[24,28]. The rapid cooling rate causes less segregation, and thus aggravates the lattice distortion inside microstructures of these additively manufactured RHEAs[66]. As shown in Fig. 8, only a few RHEAs have considerable room- and high-temperature mechanical properties under 1200 °C. These as-printed RHEAs exhibit room-temperature strength of above 2500 MPa, and their high-temperature strength can reach above 1500 MPa at 800 °C and remain at above 900 MPa under 1200 °C. This result suggests that the additively manufactured RHEAs can maintain their good mechanical properties, which are similar to or even better than those of the as-cast RHEAs.

4 Problems in Additive Manufacturing of RHEAs

Progress in exploring more complex RHEA systems and their diverse performance provides ceaseless impetus to the design and manufacture of new RHEAs[2,8,67]. RHEAs with

Table 2 Hardness of additively manufactured RHEAs

RHEA system	Method	Hardness, HV/×9.8 MPa	Ref.
$W_xMoTaNb$	LCD	476, 485, 497	[16]
WMoTaNb	SLM	826	[17]
WMoTaNb	DED	493	[18]
WMoTaNbV	SLM	664	[21]
NbMoTaTi	SLM	422	[25]
NbMoTaNi	SLM	827	[25]
NbMoTaNiTi	SLM	628	[25]
AlMoNbTa	DED	646	[28]
NbTaTiMo	SLM	452	[29]
TiZrNbHfTa	LMD	509	[31]
WMoTaNbTi	SEBM	511	[37]
WMoTaNbVFeCoCrNi	SEBM	836	[38]
NbMoTaNiCr	WAAM	911	[45]

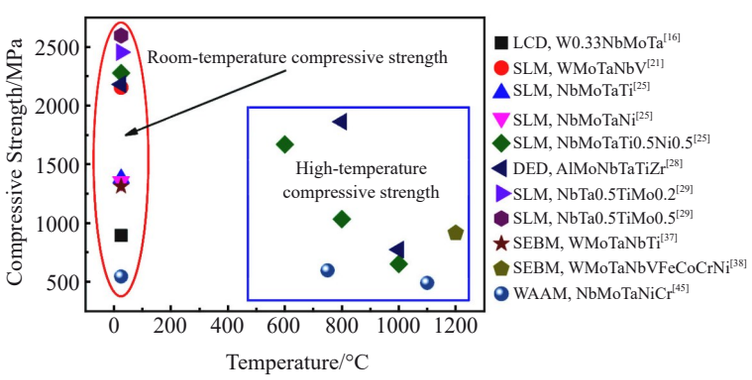

Fig.8 Compressive strength of additively manufactured RHEAs at room- and high-temperatures

excellent high-temperature mechanical behavior attract much attention[68–70]. However, the additive manufacturing techniques are influenced by the following factors: small melt pool, large thermal gradient, residual stress, and rapid cooling process. Besides, crack and pore are two common defects in additively manufactured RHEAs. The research on Ni-based superalloys clarifies that there are at least three cracking modes in the additively manufactured alloys: solidification cracking, liquation cracking, and solid-state cracks[71]. However, the cracking modes and their mechanisms are still obscure. Up to now, the solidification cracking and solid-state cracking may occur in microstructures of as-deposited RHEAs, particularly in RHEAs with intrinsic brittleness, such as WMoTaNb-based RHEAs[38]. Therefore, the characterization, identification, and formation mechanism of these cracking modes in additively manufactured RHEAs[14,18–19,21] should be further researched.

Melia et al[18] noticed that the cracks are suppressed in the regions with dense cellular structures (Fig. 9a). Moorehead et al[19] applied the high-throughput additive manufacturing on WMoTaNb RHEA, and found the effective cracking suppression method with cellular structures (Fig. 9a$_1$). Yang et al[72] reported the similar results: the cellular structures induce the substantially cracking suppression effect in the as-deposited $Ni_6Cr_4WFe_9Ti$ alloy with good mechanical performance (Fig. 9b and 9c). Therefore, it can be concluded that cracking in additively manufactured RHEAs can be effectively reduced by forming substructures (Fig. 9d–9g). For example, the additively manufactured $Ni_6Cr_4WFe_9Ti$ alloy shows excellent room-temperature tensile ductility and strength, which is based on the superb ductility of WNiFe alloys[73–74]. It should be noted that the enhancement in

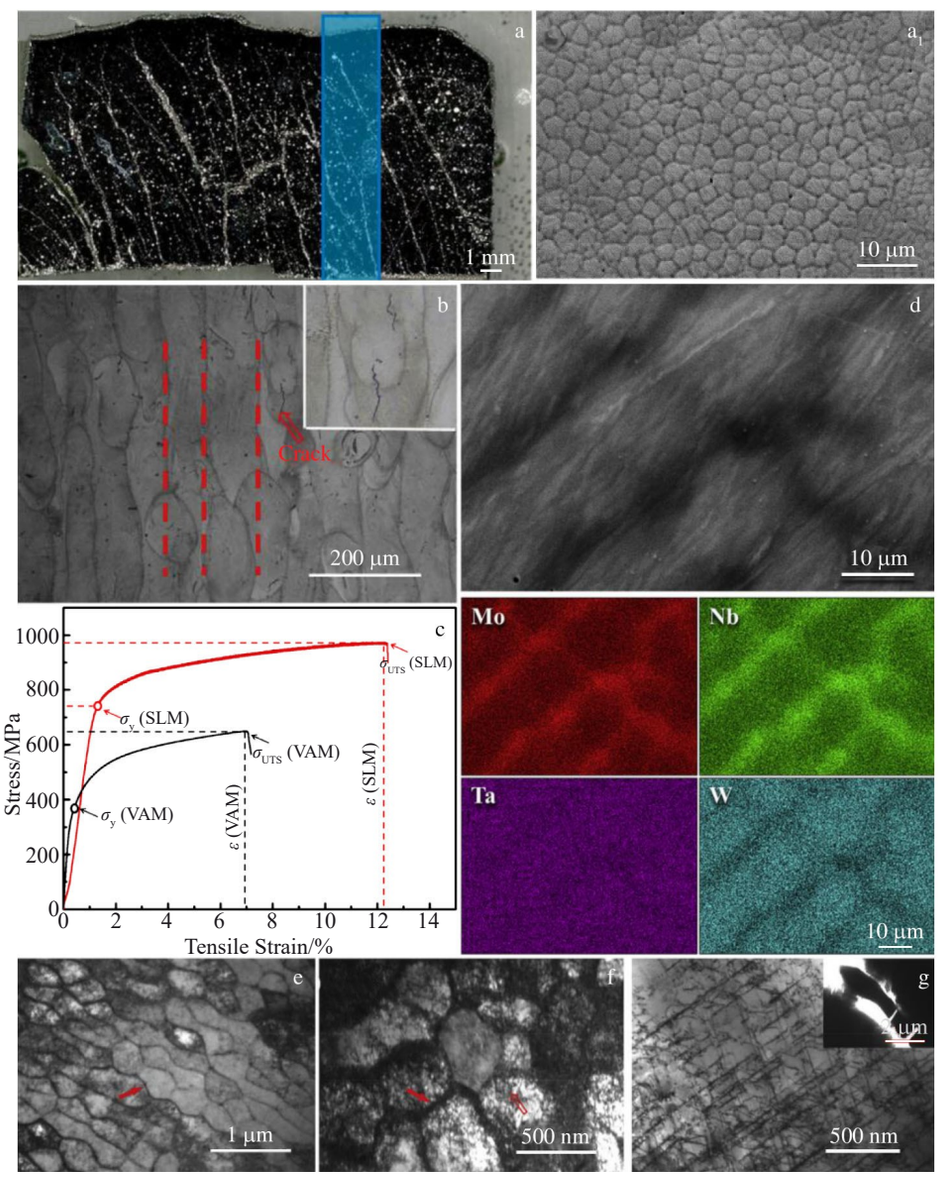

Fig.9 Cracking suppression in RHEAs: (a) cracks[18] and (a$_1$) cellular structures[19] in WMoTaNb RHEA; (b) cracking microstructure and (c) mechanical properties of Ni6Cr4WFe9Ti alloy[72]; (d – g) microstructures and element distributions of cellular structures and dislocations in cellular structures[72]

printability of RHEAs should not influence their mechanical performance. In this case, the additively manufactured $Ni_6Cr_4WFe_9Ti$ alloy exhibits good ductility and printable performance.

Nowadays, numerous RHEAs with diverse performances have been investigated, the additive manufacturing techniques can accelerate the processing speed, and almost all kinds of complex parts can be designed by computer. However, not all RHEAs have good printability. Searching for suitable additive manufacturing techniques for specific RHEAs is of great importance.

5 Summary and Outlook

Refractory high-entropy alloys (RHEAs), such as WMoTaNb-based and NbZrTi-based RHEAs, have excellent mechanical behavior at high-temperatures. With the development in the application requirements of aerospace, nuclear, and power plant, RHEAs with complex geometries are of great importance. In recent years, numerous RHEAs have been designed, but only a few RHEAs are printable. Among the commonly used additive manufacturing techniques, the selected laser melting, direct energy deposition, selective electron beam melting, and wire arc additive manufacturing are representative methods to fabricate RHEAs. The WMoTaNb-based RHEAs have intrinsic cracking and pores, which can hardly be suppressed. In contrast, the NbZrTi-based RHEAs have good room-temperature ductility and printability. The better the ductility, the better the printability.

The amelioration methods, alteration of intrinsic ductility of brittle alloys, and modification of printability provide new insights for the development of RHEAs with good printability.

References

1 Lee C, Maresca F, Feng R *et al*. *Nature Communications*[J], 2021, 12(1): 5474

2 Xiong W, Guo A X Y, Zhan S *et al*. *Journal of Materials Science and Technology*[J], 2023, 142: 196

3 Senkov O N, Wilks G B, Miracle D B *et al*. *Intermetallics*[J], 2010, 18(9): 1758

4 Senkov O N, Wilks G B, Scott J M *et al*. *Intermetallics*[J], 2011, 19(5): 698

5 Senkov O N, Woodward C F. *Materials Science and Engineering A*[J], 2011, 529: 311

6 Liu C J, Gadelmeier C, Lu S L *et al*. *Acta Materialia*[J], 2022, 237: 118 188

7 Kalali D G, Antharam S, Hasan M *et al*. *Materials Science and Engineering A*[J], 2021, 812: 141 098

8 Wang Z C, Chen S Y, Yang S L *et al*. *Journal of Materials Science and Technology*[J], 2023, 151: 41

9 Roh A, Kim D, Nam S *et al*. *Journal of Alloys and Compounds*[J], 2020, 822: 153 423

10 Frazier W E. *Journal of Materials Engineering and Performance*[J], 2014, 23: 1917

11 Bermingham M J, Stjohn D H, Krynen J *et al*. *Acta Materialia*[J], 2019, 168: 261

12 Galati M, Iuliano L. *Additive Manufacturing*[J], 2018, 19: 1

13 Kunce I, Polanski M, Bystrzycki J. *International Journal of Hydrogen Energy*[J], 2014, 39(18): 9904

14 Dobbelstein H, Thiele M, Gurevich E L *et al*. *Physics Procedia*[J], 2016, 83: 624

15 Zhang H, Xu W, Xu Y J *et al*. *The International Journal of Advanced Manufacturing Technology*[J], 2018, 96: 461

16 Li Q Y, Zhang H, Li D C *et al*. *Materials*[J], 2019, 12(3): 533

17 Zhang H, Zhao Y Z, Huang S *et al*. *Materials*[J], 2019, 12(5): 720

18 Melia M A, Whetten S R, Puckett R *et al*. *Applied Materials Today*[J], 2020, 19: 100 560

19 Moorehead M, Bertsch K, Niezgoda M *et al*. *Materials and Design*[J], 2020, 187: 108 358

20 Huber F, Bartels D, Schmidt M. *Materials*[J], 2021, 14: 3095

21 Gu P F, Qi T B, Chen L *et al*. *International Journal of Refractory Metals and Hard Materials*[J], 2022, 105: 105 834

22 Xu J T, Duan R, Feng K *et al*. *Additive Manufacturing Letters*[J], 2022, 3: 100 079

23 Chen L, Yang Z W, Lu L K *et al*. *Journal of Refractory Metals and Hard Materials*[J], 2023, 110: 106 027

24 Dobbelstein H, Gurevich E L, George E P *et al*. *Additive Manufacturing*[J], 2019, 25: 252

25 Zhang H, Zhao Y Z, Cai J L *et al*. *Materials and Design*[J], 2021, 201: 109 462

26 Wang H, Gould B, Moorehead M *et al*. *Journal of Materials Processing Technology*[J], 2022, 299: 117 363

27 Feng J Y, Wei D X, Zhang P L *et al*. *Journal of Manufacturing Processes*[J], 2023, 85: 160

28 Su B, Li J, Yang C *et al*. *Materials Letters*[J], 2023, 335: 133 748

29 Wang F, Yuan T C, Li R D *et al*. *International Journal of Refractory Metals and Hard Materials*[J], 2023, 111: 106 107

30 Dobbelstein H, George E P, Gurevich E L *et al*. *International Journal of Extreme Manufacturing*[J], 2021, 3(1): 15 201

31 Dobbelstein H, Gurevich E L, George E P *et al*. *Additive Manufacturing*[J], 2018, 24: 386

32 Li N, Wang R X, Zhao H B *et al*. *Materials Today Communications*[J], 2022, 32: 103 847

33 Yu T, Wang H Q, Han K *et al*. *Intermetallics*[J], 2022, 149: 107 669

34 Zhao Y, Wu M F, Jiang P C *et al*. *Journal of Materials Research and Technology*[J], 2022, 20: 1908

35 Xiao B, Jia W P, Tang H P *et al*. *Additive Manufacturing*[J], 2022, 54: 102 738

36 Popov V V, Katz-Demyanetz A, Koptyug A *et al*. *Heliyon*[J], 2019, 5: e01188

37 Xiao B, Jia W P, Tang H P *et al*. *Journal of Materials Science and Technology*[J], 2022, 108: 54

38 Xiao B, Jia W P, Wang J *et al*. *Materials Characterization*[J],

2022, 193: 112 278
39 Rodrigues T A, Duarte V, Miranda R M *et al*. *Materials*[J], 2019, 12(7): 1121
40 Williams S W, Martina F, Addison A C *et al*. *Materials Science and Technology*[J], 2016, 32: 641
41 Ding D H, Pan Z X, Cuiuri D *et al*. *The International Journal of Advanced Manufacturing Technology*[J], 2015, 81(1–4): 465
42 Islam S, Seo G J, Ahsan M R U *et al*. *International Journal of Refractory Metals and Hard Materials*[J], 2023, 110: 106 042
43 Marinelli G, Martina F, Lewtas H *et al*. *Journal of Nuclear Materials*[J], 2019, 522: 45
44 Liu J, Li J, Du X *et al*. *Materials*[J], 2021, 14(16): 4512
45 Huang S F, Zeng X L, Du X *et al*. *Vacuum*[J], 2023, 210: 111 900
46 Taminger K M B, Hafley R A. *3rd Annual Automotive Composites Conference*[C]. Troy: Society of Plastic Engineers, 2003: 9
47 Mok S H, Bi G J, Folkes J *et al*. *Surface and Coatings Technology*[J], 2008, 202(16): 3933
48 Martina F, Mehnen J, Williams S W. *Journal of Materials Processing Technology*[J], 2012, 212: 1377
49 DebRoy T, Wei H L, Zuback J S *et al*. *Progress in Materials Science*[J], 2018, 92: 112
50 Wang X C, Laoui T, Bonse J *et al*. *The International Journal of Advanced Manufacturing Technology*[J], 2002, 19: 351
51 Moghaddam A O, Shaburova N A, Samoduroyva M N. *Journal of Materials Science and Technology*[J], 2021, 77: 131
52 Senkov O N, Scott J M, Senkova S V *et al*. *Journal of Alloys and Compounds*[J], 2011, 509(20): 6043
53 Senkov O N, Scott J M, Senkova S V *et al*. *Journal of Materials Science*[J], 2012, 47: 4062
54 Ouyang D, Zhang P C, Zhang C *et al*. *Materials Science and Engineering A*[J], 2023, 867: 144 745
55 Gou S Y, Gao M Y, Shi Y Z *et al*. *Acta Materialia*[J], 2023, 248: 118 781
56 Kou S. *Acta Materialia*[J], 2015, 88: 366
57 Lu N N, Lei Z L, Hu K. *Additive Manufacturing*[J], 2020, 34: 101 228
58 Schuh B, Völker B, Todt J *et al*. *Acta Materialia*[J], 2018, 142: 201
59 Lilensten L, Couzinië J P, Perriére L *et al*. *Acta Materialia*[J], 2018, 142: 131
60 Huang R, Wang W, Li T X *et al*. *Journal of Alloys and Compounds*[J], 2023, 940: 168 821
61 Huang W J, Hou J X, Wang X J *et al*. *Intermetallics*[J], 2022, 151: 107 735
62 Qi L, Chrzan D C. *Physical Review Letters*[J], 2014, 112: 115 503
63 Sheikh S, Shafeie S, Hu Q *et al*. *Journal of Applied Physics*[J], 2016, 120(16): 164 902
64 Han Z D, Luan H W, Liu X *et al*. *Materials Science and Engineering A*[J], 2018, 712: 380
65 Pan J Y, Dai T, Lu T *et al*. *Materials Science and Engineering A*[J], 2018, 738: 362
66 Chen H, Kauffmann A, Laube S *et al*. *Metallurgical and Materials Transactions A*[J], 2018, 49: 772
67 Tian Y S, Zhou W Z, Tan Q B *et al*. *Transactions of Nonferrous Metals Society of China*[J], 2022, 32(11): 3487
68 Xie X C, Li N, Liu W *et al*. *Chinese Journal of Mechanical Engineering*[J], 2022, 35(1): 142
69 Senkov O N, Miracle D B, Chaput K J *et al*. *Journal of Materials Research*[J], 2018, 33(19): 3092
70 Guan S, Ren J, Mooraj S *et al*. *Journal of Phase Equilibria and Diffusion*[J], 2021, 42(5): 748
71 Tang Y T, Panwisawas C, Ghoussoub J N *et al*. *Acta Materialia*[J], 2021, 202: 417
72 Yang X G, Zhou Y, Xi S Q *et al*. *Materials Science and Engineering A*[J], 2019, 767: 138 394
73 Iveković A, Montero-Sistiaga M L, Vanmeensel K *et al*. *International Journal of Refractory Metals and Hard Materials*[J], 2019, 82: 23
74 Ye H, Huang Y B, Wei C *et al*. *Journal of Alloys and Compounds*[J], 2022, 909: 164 684

增材制造难熔高熵合金综述

肖　邦[1,2]，贾文鹏[1]，王　建[1]，周　廉[1,2]
(1. 西北有色金属研究院 金属多孔材料国家重点实验室，陕西 西安 710016)
(2. 西北工业大学 凝固技术国家重点实验室，陕西 西安 710072)

摘　要：寻求可打印金属材料的研究至关重要。近年来，多种可打印性良好的材料已被发掘出来，如Ti-6Al-4V、FeMnCoCrNi、不锈钢及一些难熔高熵合金。尽管已经获得了诸多可喜结果，增材制造难熔高熵合金依然发展缓慢。由于难熔高熵合金的优越高温性能，复杂成形的需求也日渐高涨。本文主要介绍了增材制造难熔高熵合金的一些研究进展，综述了有关难熔高熵合金激光增材制造、电子束增材制造和丝材增材制造技术，并为后续研究工作提供参考。此外，本文也系统地讨论了有关增材制造难熔高熵合金面临的机遇和挑战。

关键词：增材制造；难熔高熵合金；激光沉积系统；电子束熔化系统；组织；力学性能

作者简介：肖　邦，男，1991年生，博士生，西北工业大学凝固技术国家重点实验室，陕西 西安 710072，电话：029-86231095，E-mail：ninxbnwpu@163.com